IAES International Journal of Robotics and Automation (IJRA)
Vol. 15, No. 1, March 2026, pp. 181~189
ISSN: 2722-2586, DOI: 10.11591/ijra.v15i1.pp181-189

Design and drag force analysis of an autonomous underwater remotely operated vehicles for coral reef health assessment

Pandiyarajan Rajendran, Srinivasan Alavandar
Department of Mechatronics Engineering, Agni College of Technology, Chennai, India

Article Info

Article history:

Received Jun 26, 2025
Revised Dec 3, 2025
Accepted Dec 15, 2025

Keywords:

Autonomous
Light detection and ranging
Navigation
Remotely operated vehicles
Underwater

ABSTRACT

This research presents the conception and building of an inexpensive remotely operated vehicle (ROV) system to ease the tasks of underwater inspection and environmental monitoring in areas where the global positioning system (GPS) signal is not available. A Raspberry Pi-based control unit, an inertial measurement unit (IMU), and depth sensors are merged in the system so that simple data acquisition and remote operation can be carried out. ROV hydrodynamic drag and stability for a state of ideal balance and maneuverability were assessed through tests based on preliminary simulations in Fusion 360 and empirical calculations. The ROV is confirmed to be behaving as expected in terms of stability, imaging capabilities, and responsiveness to operator control in the testing that was done in controlled water environments. This paper, the work, and the testing, in fact, present the initial design, but it is a significant step towards the consideration of the possible further embedding of autonomous features "simultaneous localization and mapping (SLAM)-based navigation, doppler velocity log (DVL), light detection and ranging (LiDAR) systems" for completely autonomous underwater guided missions.

Corresponding Author:

Pandiyarajan Rajendran
Department of Mechatronics Engineering, Agni College of Technology
Thalambur, Chennai, Tamilnadu, India, 600130
Email: pandiyan.rajan8@gmail.com

1. INTRODUCTION

Remotely operated vehicles (ROVs) are major components in marine research of the modern era, changing the way underwater exploration, inspection, and maintenance are done in sectors such as offshore energy, naval defense, oceanographic research, and environmental monitoring [1]. ROVs' abilities to function in difficult and deep-sea conditions make it possible to carry out subsea infrastructure inspections, coral reef health assessments, and marine biodiversity monitoring in a safe and exact way that operations which would inherently be very dangerous for human divers [2]–[5]. Specifically, inexpensive ROVs have been instrumental in making marine technology more accessible to small research institutions and environmental organizations which in turn have been able to carry out routine surveys and ecological monitoring of the like of coral reefs that are sensitive habitats. These are ecosystems that not only provide the greatest variety of life but also act as natural barriers against coastal erosion and thus need to be continuously monitored for coral bleaching, pollution, and habitat degradation. One of the major focuses of recent underwater robotic advances is the use of various technologies such as acoustic sensing, sensor fusion, and machine vision to increase autonomy, imaging resolution, and environmental awareness [6]–[10]. Modular and open-source adaptable platforms such as BlueROV2 and OpenROV have gained traction both in the academic and commercial sectors; however, they are usually costly or require advanced skills for customization [11]–[14]. The main research problem is to find the best compromise between cost,

performance, and system reliability, especially in navigation and control systems. It is stated that high-end navigation instruments like doppler velocity logs (DVLs) and light detection and ranging (LiDAR) sensors can improve localization accuracy, but their costs make them less feasible for small-scale research and educational applications [15]–[18]. In the same way, the installation of heavy and power-consuming onboard computing units limits the battery life and the mobility of low-cost systems.

In response to these issues, the study demonstrates the development and initial testing of a cheap underwater robot (ROV) platform, mainly made for coral reef monitoring and shallow-water environmental research. The device architecture features a Raspberry Pi-based main unit linked with an inertial measurement unit (IMU) and depth sensor for automated navigation and recording of environmental data. To aid the design of smooth underwater operations at shallow depths, first-pass calculations of hydrodynamic drag and stability were carried out in fusion 360 and through empirical methods. Verification of the underwater vehicle's equilibrium, recording quality, and agility were done through experiments in water tanks or other suitable controlled aquatic environments. This hardware setup creates a versatile base layer, which can be layered by further research and development of advanced autonomy features, such as simultaneous localization and mapping (SLAM), sensor fusion, and adaptive control, thus effectively closing the cost-performance efficiency gap in underwater robotics.

This research is centered around the problem of how to create underwater systems that are able to operate independently and efficiently in changing aquatic environments. The primary task is to engineer, build, and then prove the feasibility of a self-reliant underwater robotic vehicle of the future. A prototype capable of performing the intended functions was put together with a mini-Raspberry Pi computing platform, which was combined with proportional integral derivative (PID) control algorithms and simultaneous localization, and mapping (SLAM) was used for autonomous navigation. The experiment method was a series of learning cycles, each time the virtual design, prototyping, sensor integration, and calibration were followed by testing both in the laboratory and open-sea. The outcomes were in agreement with the hypotheses of efficient multi-sensor fusion, smooth mechanical-electrical-computational integration, and fast real-time data processing (42 frames per second) through parallel computing.

2. METHOD

2.1. Electronic design

The Pixhawk flight controller is at the heart of the proposed underwater remotely operated vehicle. It is a controller that works with integrated sensors, electronic speed controllers (ESCs), and a digital camera setup. Pixhawk is the one that takes care of processing all the sensor data it gets. It controls the brushless direct current (BLDC) motors through those ESCs in a very efficient manner. In fact, it is the same unit that also handles real-time video transmission without any issues.

Wireless communication ensures that the remote control is always smooth and very much responsive. It also provides clear feedback during operations at all times. The commands are initiated at the transmitter and are followed up by the flight controller receiving them. After processing the commands, the flight control system is the one that actually carries out the instructions. The whole system has the capability of operating eight BLDC motors. Four of them are at the corners for lateral movement while the other four are positioned centrally for vertical thrust and directional control. Such a setup is all about precise and stable underwater navigation. Moreover, it still maintains its energy efficiency even in the most challenging situations. Figure 1 illustrates the electronic design of the vehicle and remote system.

2.2. Design and construction of the ROV

The remotely operated vehicle (ROV) was a compact and hydrodynamically stable unit with a streamlined structure of 58.6 cm length, 42.21 cm width, and 32.61 cm height. The dimensions chosen allow a good mix of buoyancy, maneuverability and payload capacity so as to be able to work efficiently in canoe-type shallow-water coral reef environments where there is less space and a need for precise movement control due to the fragile ecosystems [20]. The propulsion system is made up of five brushless direct current (DC) motors (XCSOURCE QF-2611, 4500 kV, three-phase) whose revolutions per minute (RPMs) are regulated by ESC30A speed controllers capable of delivering up to 30 A. Each one of the four thrusters is at 45° angles with respect to a corner of the frame and the vectorized thrust distribution thus achieved is used in this work to realize smooth omnidirectional motion-forward, backward, lateral, and rotational (yaw)-without the need of extra mechanical linkages [21].

Such a set-up improves the robot's maneuvering ability and stability in a turbulent flow of air or water at the inspection site, a place where, in general, coral structures are found and the user's task is to perform the inspection from close proximity. The vertically oriented fifth thruster that is located centrally on the top section of the body adds heave (up–down) control to the system, enabling depth stability, and at the

same time buoyancy changes, if any, can be taken care of during sampling or imaging operations with the help of this thruster [22]. We arrived at the ideal frame geometry and thruster placement after empirical balance and drag simulations for which we used fusion 360 and thus made sure that center of gravity (CG) and center of buoyancy (CB) were not only vertically aligned but also were at a point from where stable hovering would be possible. We also factored in the MPU6050 inertial measurement unit (IMU) which, along with a complementary filter, gives real-time three-dimensional orientation support for the stabilization and attitude correction functions performed during remote operation. Figure 2 shows the ROV's computer-aided design (CAD) model and the corresponding experiment prototype.

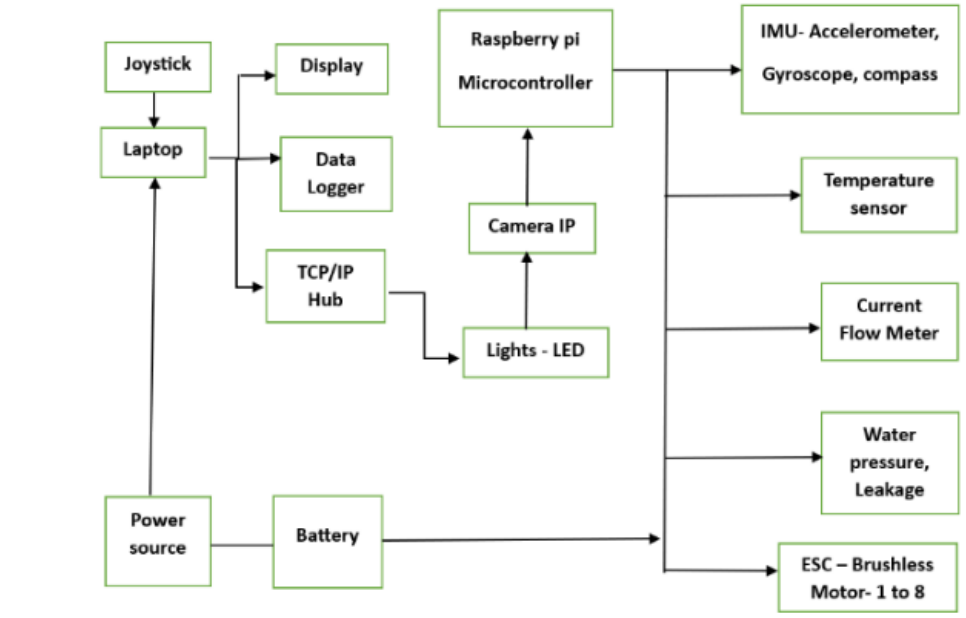

(a)

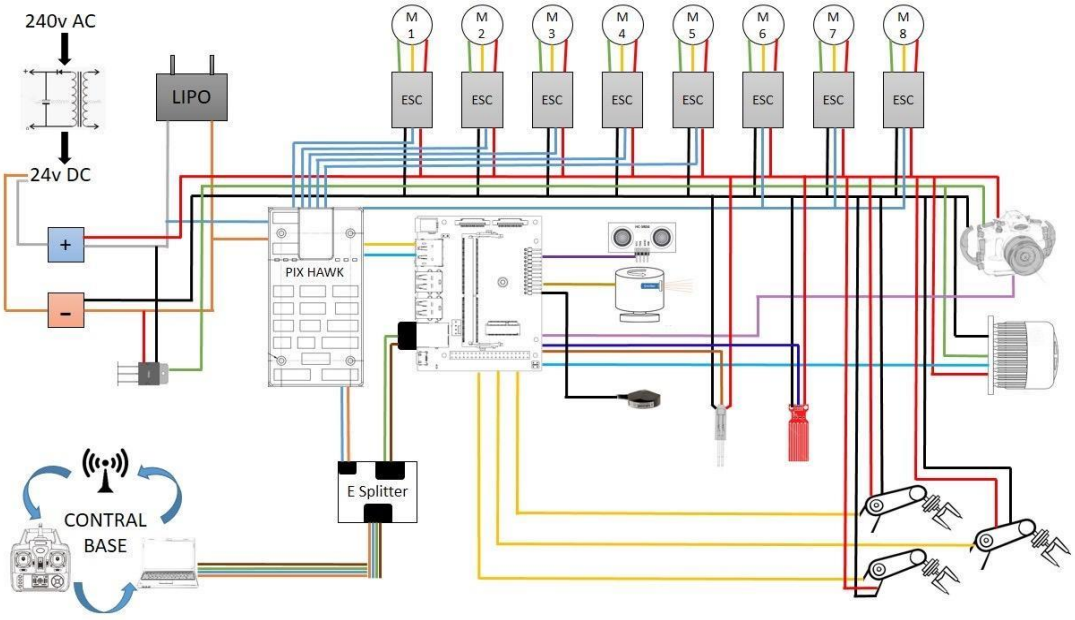

(b)

Figure 1. On-vehicle and remote system: (a) block diagram of ROV system and (b) electrical circuit connections

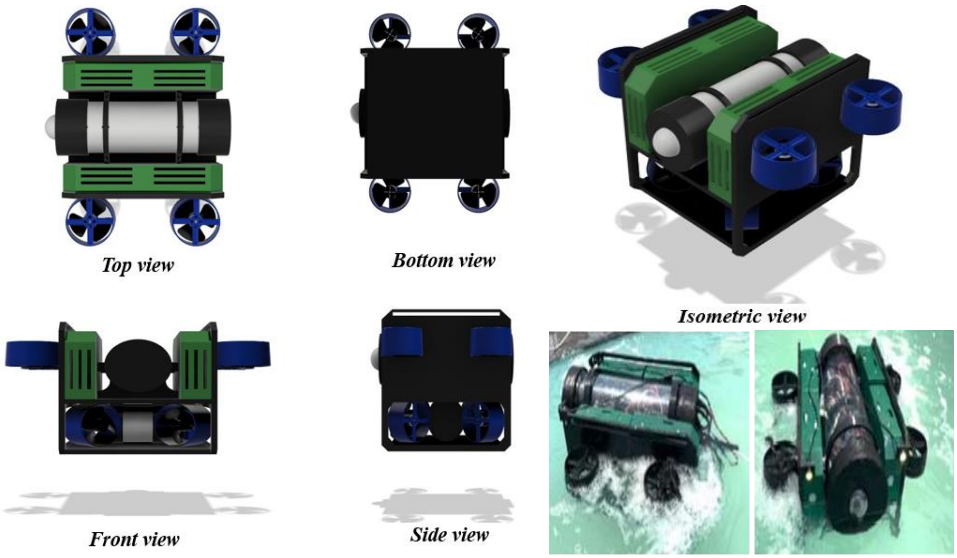

Figure 2. CAD model of the underwater rover and experimental image

2.3. Navigation system

The system of navigation consists of:

- Four propellers for controlling the vehicle in the planes and one propeller for vertical movement.
- MPU6050 motion sensor for monitoring orientation in real time.

To hamper the opposition of forces, the propellers are well placed along the vehicle. The guidance system solves the directional force vectors based on the kinematic models of the omni-wheel robot, providing exact and easy motion. Sensors of depth and pressure have been integrated to work in high efficiency underwater up to 100 meters deep [23].

2.4. Communication system

The ROV communicates with the remote operator enabling the high-speed, noise-resistant data transfer through fiber-optic cables that allow signals to be transmitted without damage over long distances [24]. Notwithstanding the idealness of fiber optics, the first model utilizes the transmission control protocol/ internet protocol (TCP/IP)-based ethernet cable communication for a distance of 100 meters. This arrangement of instruments not only supports the instantaneous exchange of data but also transfers the video from the operator station to the onboard processing unit.

2.5. Weight evaluation

The remotely operated vehicle (ROV) is expressly designed to function efficiently and with considerable stability at a depth that is below the surface of the water. The center of buoyancy should be located above the center of mass to ensure stability, which is a priority design concept. The buoyant tank is placed on the top of the ROV, and the weight elements are positioned at the bottom for a better center of gravity. The main linking elements of the ROV are galvanized pipes; the construction of the ROV involved the use of eight elbow connectors and fourteen pipes. For producing the floatable part of the submarine, fiberglass is preferred. By solving the system of (1) and (2), the ROV's weight, displacement, center of buoyancy, and center of gravity are determined. The weight of the pipes is calculated as the product of their material volume and specific weight, which is stated in (1),

$$W_{pipe} = \pi \times p_{material} \times L \times (D_{out}^2 - D_{in}^2) \quad (1)$$

where D_{out}^4 and D_{in}^4 are the outer and inner diameters of the pipe; L is the length of the tube; and ρ is the specific weight of the pipe material. The extra weight that is carried inside the pipes by the water ballast can be found using (2).

$$W_{ballast} = \pi \times p_{water} \times L \times D_{in}^2 \times h \quad (2)$$

where y is the depth of water in the pipe and λ is the specific weight of water.

2.6. Buoyancy evaluation

In (2), D and d are the outer and inner diameters of the pipe; L is the length of the tube; and ρ is the specific weight of the pipe material. The extra weight that is carried inside the pipes by the water ballast can be found using (2), where y is the depth of water in the pipe and λ is the specific weight of water,

$$\Delta B = \pi \times p_{water} \times (\frac{D_{out}^4}{4}) \times L \quad (3)$$

$$M_x = \sum_{i=0}^{n}(X_i \times W_i + X_{ai} \times W_{ai}) \quad (4)$$

$$M_y = \sum_{i=0}^{n}(Y_i \times W_i + Y_{ai} \times W_{ai}) \quad (5)$$

$$M_z = \sum_{i=0}^{n}(Z_i \times W_i + Z_{ai} \times W_{ai}) \quad (6)$$

where, and are the weights of the components and the added ballast weights; are the components' center of gravity coordinates; are the added ballast weight coordinates. Moreover, the buoyancy moment is found by (7).

$$M_{bx} = \sum_{i=0}^{n}(X_i \times B_i) \quad (7)$$

$$\text{aa}M_{bz} = \sum_{i=0}^{n}(Z_i \times B_i) \quad (8)$$

Following these equations, the result for the total weight of the ROV is 12.17 kg. At the same time, the buoyancies and the centers of gravity are Bx=0.0 cm, By=0.0 cm, Bz=20.60 cm, and Gx=0.0 cm, Gy=0.0 cm, Gz = 13.32cm.

2.7. Moment stability evaluation

The stability of ROVs is one of the most important characteristics, and it is an indication of how well the device can recover its initial position after a tilt (trim). For an underwater vehicle to be stable, the net effect of buoyancy and gravity acting on it must be positive. It is achieved by keeping the center of buoyancy higher than the center of gravity. Which then makes the distance between the two the most when the stability is the highest. The stability of a ROV at a certain heel angle can be measured through (9).

$$M_s = W \times (B_z - G_z) \times \sin(\theta) \quad (9)$$

What is the stability moment; vehicle weight; the vehicle distance from the center of buoyancy to the center of gravity; and heel angle. The stability moment calculations are shown in Figure 3 and explained graphically.

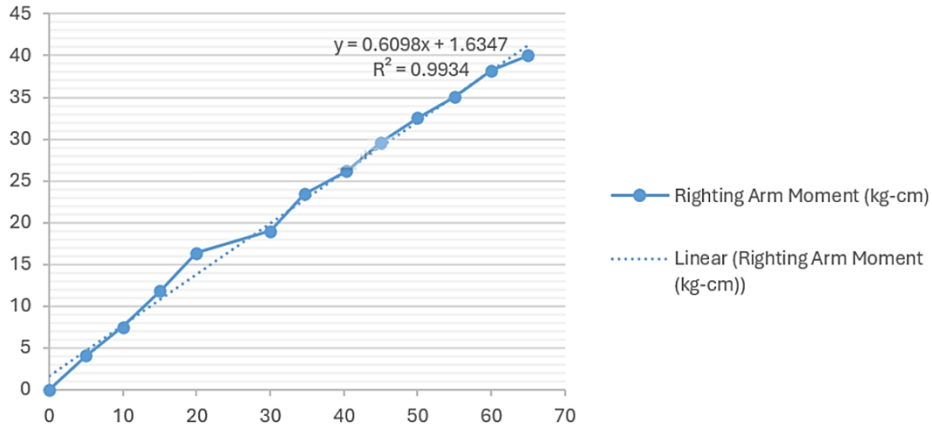

Figure 3. Stability moment

2.8. Drag force and stability analysis of the ROV

Drag force implies the negative effect that an object experiences when it moves through any fluid, such as air or water. The movement of the object in the fluid causes the force to act in the opposite direction [25]. Surface roughness, fluid density, and speed are some parameters that affect the drag force. In (10), we get the basis for the calculation of the drag force.

$$D = \left(\frac{1}{2}\right) C_d . \rho . V^2 . A \quad (10)$$

Basically, it refers to the fluid density, while: The drag coefficient, which usually is between 0.4 and 1.0 depending on the speed of the object and the different fluids being used, represents the relative velocity between the body and the fluid; and: is the projected cross-section area perpendicular to the flow direction. The length of the drag coefficient got determined from the data. The calculations in this study were made considering no heel angle change and numerical analysis of drag force at various speeds, as described in Figure 4.

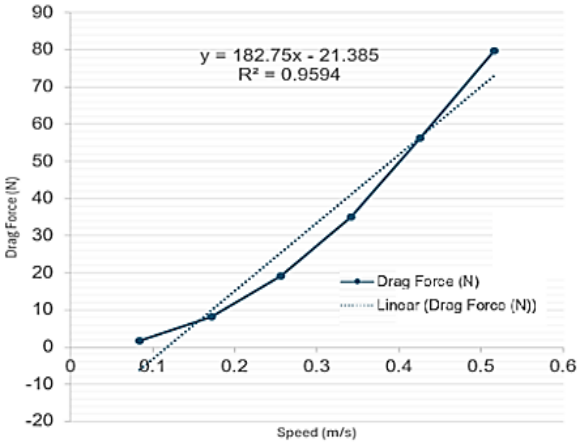

Figure 4. Drag force evaluation

3. RESULTS AND DISCUSSION

3.1. Experimental results

We have outlined the procedure followed to test the remotely operated vehicle (ROV) when the Raspberry Pi 3 was used as an onboard computer. The research also gives a clear test of the hardware resource distribution over various algorithms and processes that are working simultaneously. Moreover, the images collected from images in a controlled aquatic area and real-sea conditions are analysed. In addition to the above, the functionality of the smart PID controller is determined. At the same time, the performance of the new product is compared with that of the two known ROVs.

3.2. ROV performance

3.2.1. Motortesting

The Arduino nano microcontroller and the Ardu-Pilot development board have undergone several tests in order to decide which is the most effective way to run the brushless motors. Thus, the various kinds of controller were tested to find out which one could generate the best pulse width modulated (PWM) signal required by the ESC30A electronic speed controller. A further step to resolve this was made by designing custom software for the Arduino nano microcontroller to generate PWM signals which are of high resolution and can cope with the incessant changes in the speed of the motors. Many experiments later, the perfect PWM signal timing that lead to the best ROV stability was found to be 1 µs and was almost a thousand times faster than the original signal.

3.2.2. Temperature monitoring in Raspberry Pi 3 and ROV capsule

The temperature in the capsule is controlled by the DS18B20 digital temperature sensor which is connected to an Arduino nano microcontroller via the inter-integrated (I2C) protocol. One of the examples to evaluate the internal temperature changes of the vehicle is the motors working process to produce heat through the ESC30A speed controllers. A temperature reading of the DS18B20 sensor is executed by an internal algorithm of the Arduino nano microcontroller, and a different method was employed to track the Raspberry Pi 3's chipset temperature. In order to prevent component temperature from rising above 65 °C, it was necessary to maintain proper working temperatures. The behavior of the Raspberry Pi 3 chipset's temperature is visualized in Figure 5, as it quickly rose to 55 °C after 1 hour of continuous usage at the lowest motor speed. In the diagram, the inner capsule temperature is shown, which reached 36 °C in the same conditions. The temperature of both chips gradually decreased with time after the motors were switched off.

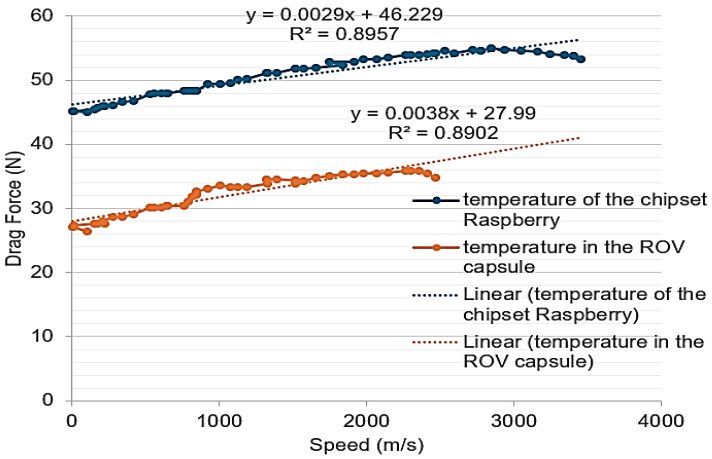

Figure 5. Temperature measurement of the chipset and the ROV capsule

3.2.3. Battery bank performance

The power consumption and the runtime of the battery banks during ROV operation are shown in Figure 6. The operation of the two battery banks was compared by simulating various scenarios.

- The 5V battery bank that was used for the supply of power to the digital components provided a continuous runtime of 500 minutes (8 hours) while executing ROV control algorithms (Figure 5).
- The 11 V battery bank, which is in charge of the ESC30A motor controllers, was about 120 minutes (2 hours) still fast enough at medium speed (Figure 6).
- The battery life was changed in accordance with the ROV navigation and propulsion needs, which could be up or down in line with the movement patterns.

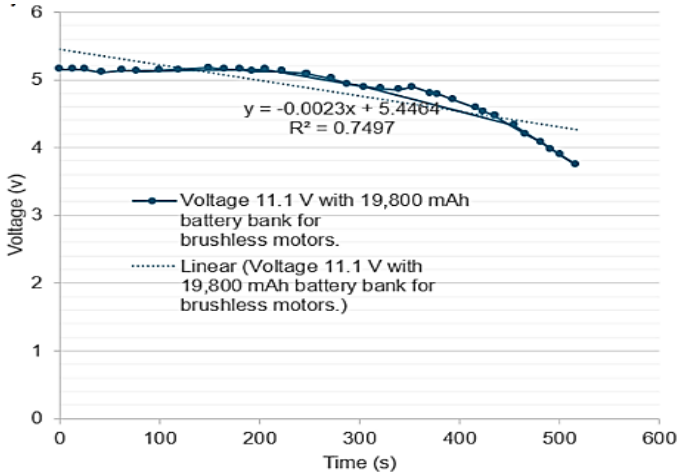

Figure 6. Battery bank behavior during ROV operation 5 V with 10,000 Mah battery bank for digital devices

3.3. Hardware resource utilization

The assignment of resources to critical processes unveils that PID 3286 (ROV parallel computing algorithm) was the one with the largest share with 76% of central processing unit (CPU) and 13.9% of random-access memory (RAM). After this, the video capture algorithm (PID 3239) consumed 39% of CPU and 11.0% of RAM, and the virtual network computing (VNC) protocol for remote access (PID 2645) used 31% of CPU and 10% of RAM. The acquired 3D position algorithm (PID 3263), the one that was in charge of the data processing from the MPU6050 sensor to visualize the 3D position of the ROV, needed 16% of CPU and 2% of RAM. The motors control algorithm (PID 1203) also showed lower resource consumption at 10% CPU and 4% RAM, and the measure temperature algorithm (PID 3223), which tracked with the DS18B20 sensor, at 8% CPU and 4% RAM. The above findings showcase the effective allocation of processing power across the various control functions, thus ensuring the stable and responsive ROV operation.

4. CONCLUSION

The ROV prototype concept, as planned, was successfully put together and tested to demonstrate its mechanical stability and functionality in the water. The design, buoyancy, and drag force analyses showed that the ROV had positive static stability, the center of buoyancy being 17.28 cm above the center of gravity, which ensured stable underwater orientation during operation. The preliminary drag analysis with fusion 360 and empirical methods made it clear that the propulsion system is capable of overcoming hydrodynamic resistance in calm water conditions, thus maneuverability can be efficient. Tests in a controlled aquatic environment showed that the ROV was able to keep steady depth and maintain its direction during simple navigation. The power profiling revealed that the ROV could be used for about two hours, which is enough for a short-duration inspection and monitoring missions.

Nevertheless, the research is confined to laboratory-scale experiments and does not take into consideration non-linear flow dynamics, turbulence, and variations in the open sea. The next step will be to equip the platform with real-time sensor fusion for adaptive control, integration of SLAM-based navigation modules, and field testing in dynamic marine environments to determine stability and autonomy over time. Hence, the current platform provides a solid base for the further development of low-cost, semi-autonomous ROVs designed for coral reef surveillance and environmental monitoring purposes.

FUNDING INFORMATION

This is part of the research project titled "Development of a next-generation autonomous underwater ROV for coral reef health monitoring in GPS-denied environments", implemented by Agni College of Technology, Thalambur, Chennai (600130), India, and funded by Indian Institute of Technology Tirupati Navavishkar I-Hub Foundation (IITTNiF) – No. IITTNiF/TPD/2024-25/P25.

AUTHOR CONTRIBUTIONS STATEMENT

This journal uses the Contributor Roles Taxonomy (CRediT) to recognize individual author contributions, reduce authorship disputes, and facilitate collaboration.

Name of Author	C	M	So	Va	Fo	I	R	D	O	E	Vi	Su	P	Fu
Pandiyarajan Rajendran	✓	✓	✓	✓	✓	✓	✓	✓		✓		✓	✓	✓
Srinivasan Alavandar	✓		✓	✓			✓			✓	✓			

C : **C**onceptualization
M : **M**ethodology
So : **So**ftware
Va : **Va**lidation
Fo : **Fo**rmal analysis
I : **I**nvestigation
R : **R**esources
D : **D**ata Curation
O : Writing - **O**riginal Draft
E : Writing - Review & **E**diting
Vi : **Vi**sualization
Su : **Su**pervision
P : **P**roject administration
Fu : **Fu**nding acquisition

CONFLICT OF INTEREST STATEMENT

The authors declare that they have no known competing financial interests or personal relationships that could have appeared to influence the work reported in this paper. Authors state no conflict of interest.

DATA AVAILABILITY

Data availability is not applicable to this paper as no new data were created or analyzed in this study.

REFERENCES

[1] Y. Watanabe *et al.*, "Conceptual design of navigation of an AUV for monitoring CCS site at deep sea bottom," in *Volume 5: Ocean Space Utilization; Ocean Renewable Energy*, Jan. 2011, pp. 121–128. doi: 10.1115/OMAE2011-49812.

[2] G. Ferri, A. Munafo, and K. D. Lepage, "An autonomous underwater vehicle data-driven control strategy for target tracking," *IEEE Journal of Oceanic Engineering*, vol. 43, no. 2, pp. 323–343, Apr. 2018, doi: 10.1109/JOE.2018.2797558.

[3] J. K. Choi, T. Yokobiki, and K. Kawaguchi, "Peer-reviewed technical communication," *IEEE Journal of Oceanic Engineering*, vol. 43, no. 3, pp. 665–676, 2018, doi: 10.1109/JOE.2017.2735598.

[4] R. Wang and G. Chen, "Design and experimental research of underwater maintenance vehicle for seabed pipelines," in *2018 3rd International Conference on Robotics and Automation Engineering (ICRAE)*, Nov. 2018, pp. 146–149. doi: 10.1109/ICRAE.2018.8586764.

[5] H. P. Oliveira, A. J. Sousa, A. P. Moreira, and P. J. Costa, *Modeling and assessing of omni-directional robots with three and four wheels*. United Kingdom: INTECH Open Access Publisher, 2009.

[6] B. Meyer, K. Ehlers, C. Osterloh, and E. Maehle, "Smart-E an autonomous omnidirectional underwater robot," *Paladyn, Journal of Behavioral Robotics*, vol. 4, no. 4, pp. 204–210, Jan. 2013, doi: 10.2478/pjbr-2013-0015.

[7] N. H. Tehrani, M. Heidari, Y. Zakeri, and J. Ghaisari, "Development, depth control and stability analysis of an underwater remotely operated vehicle (ROV)," in *IEEE ICCA 2010*, Jun. 2010, pp. 814–819. doi: 10.1109/ICCA.2010.5524051.
[8] R. M. F. Gomes, A. Martins, A. Sousa, J. B. Sousa, S. L. Fraga, and F. L. Pereira, "A new ROV design: issues on low drag and mechanical symmetry," in *Europe Oceans 2005*, 2005, pp. 957-962 Vol. 2. doi: 10.1109/OCEANSE.2005.1513186.
[9] R. Barua, S. Mandal, and S. Mandal, "Motion analysis of a mobile robot with three omni-directional wheels," *International Journal of Innovative Science, Engineering and Technology*, vol. 2, no. 11, pp. 644–648, 2015.
[10] J. Aparicio, A. Jimenez, F. J. Alvarez, D. Ruiz, C. De Marziani, and J. Urena, "Characterization of an underwater positioning system based on GPS surface nodes and encoded acoustic signals," *IEEE Transactions on Instrumentation and Measurement*, vol. 65, no. 8, pp. 1773–1784, Aug. 2016, doi: 10.1109/TIM.2016.2552699.
[11] P. Mayer, M. Magno, and L. Benini, "Self-sustaining acoustic sensor with programmable pattern recognition for underwater monitoring," *IEEE Transactions on Instrumentation and Measurement*, vol. 68, no. 7, pp. 2346–2355, Jul. 2019, doi: 10.1109/TIM.2018.2890187.
[12] Q. Li, Y. Ben, S. M. Naqvi, J. A. Neasham, and J. A. Chambers, "Robust Student's t-based cooperative navigation for autonomous underwater vehicles," *IEEE Transactions on Instrumentation and Measurement*, vol. 67, no. 8, pp. 1762–1777, Aug. 2018, doi: 10.1109/TIM.2018.2809139.
[13] J. S. Cely, R. Saltaren, G. Portilla, O. Yakrangi, and A. Rodriguez-Barroso, "Experimental and computational methodology for the determination of hydrodynamic coefficients based on free decay test: application to conception and control of underwater robots," *Sensors*, vol. 19, no. 17, pp. 1–24, Aug. 2019, doi: 10.3390/s19173631.
[14] A. Martorell-Torres, M. Massot-Campos, E. Guerrero-Font, and G. Oliver-Codina, "Xiroi ASV: a modular autonomous surface vehicle to link communications," *IFAC-PapersOnLine*, vol. 51, no. 29, pp. 147–152, 2018, doi: 10.1016/j.ifacol.2018.09.484.
[15] R. Xu, G. Tang, D. Xie, D. Huang, and L. Han, "Underactuated tracking control of underwater vehicles using control moment gyros," *International Journal of Advanced Robotic Systems*, vol. 15, no. 1, pp. 1–8, Jan. 2018, doi: 10.1177/1729881417750759.
[16] Y.-H. Lin, S.-Y. Chen, and C.-H. Tsou, "Development of an image processing module for autonomous underwater vehicles through integration of visual recognition with stereoscopic image reconstruction," *Journal of Marine Science and Engineering*, vol. 7, no. 4, pp. 1–42, Apr. 2019, doi: 10.3390/jmse7040107.
[17] J. Jia-jia, W. Xian-quan, D. Fa-jie, F. Xiao, Y. Han, and H. Bo, "Bio-inspired steganography for secure underwater acoustic communications," *IEEE Communications Magazine*, vol. 56, no. 10, pp. 156–162, Oct. 2018, doi: 10.1109/MCOM.2018.1601228.
[18] C. S. Chin *et al.*, "System design of underwater battery power system for marine and offshore industry," *Journal of Energy Storage*, vol. 21, pp. 724–740, Feb. 2019, doi: 10.1016/j.est.2019.01.007.
[19] X. Cufí *et al.*, "EDUROVs: a low-cost and sustainable remotely operated vehicles educational program," *Sustainability*, vol. 13, no. 15, pp. 1–12, Aug. 2021, doi: 10.3390/su13158657.
[20] G. Antonelli, "On the use of adaptive or integral actions for six-degrees-of-freedom control of autonomous underwater vehicles," *IEEE Journal of Oceanic Engineering*, vol. 32, no. 2, pp. 300–312, Apr. 2007, doi: 10.1109/JOE.2007.893685.
[21] V. Utkin, A. Poznyak, Y. Orlov, and A. Polyakov, "Conventional and high order sliding mode control," *Journal of the Franklin Institute*, vol. 357, no. 15, pp. 10244–10261, Oct. 2020, doi: 10.1016/j.jfranklin.2020.06.018.
[22] R. Wernli, "The present and future capabilities of deep ROVs," *Marine Technology Society Journal*, vol. 33, no. 4, pp. 26–40, 2000.
[23] B. T. Phillips, N. Chaloux, R. Shomberg, A. Muñoz-Soto, and J. Owens, "The fiber optic reel system: A compact deployment solution for tethered live-telemetry deep-sea robots and sensors," *Sensors*, vol. 21, no. 7, pp. 1–10, Apr. 2021, doi: 10.3390/s21072526.
[24] R. Capocci, G. Dooly, E. Omerdić, J. Coleman, T. Newe, and D. Toal, "Inspection-class remotely operated vehicles-A review," *Journal of Marine Science and Engineering*, vol. 5, no. 1, pp. 1–32, Mar. 2017, doi: 10.3390/jmse5010013.
[25] R. Pandiyarajan and A. Nazhurudeen, "A study on integration of lightweight composite materials in autonomous ROVs for coral reef surveillance," *Research in Materials Science*, vol. 1, no. 1, Jan. 2025, doi: 10.1080/30654327.2025.2549246.

BIOGRAPHIES OF AUTHORS

Pandiyarajan Rajendran Professor and Head of Mechatronics Engineering at Agni College of Technology, Chennai, holds a Ph.D. in Engineering with over a decade of teaching and research experience. His expertise spans welding, materials science, robotics, and automation. His current research focuses on underwater robotics, autonomous systems, and smart sensor-based control engineering. He can be contacted at pandiyan.rajan8@gmail.com.

Srinivasan Alavandar is a distinguished academic with a Ph.D. in Intelligent Control and Robotics from IIT Roorkee. His extensive career spans over 13 years, serving in roles like Principal, Professor, and Dean Academics in leading engineering institutions. His core research expertise lies in computational intelligence, robotics, and intelligent control systems. He can be contacted at seenu.phd@gmail.com.